Supporting Information Cover Sheet

Adsorption of Polycyclic Aromatic Hydrocarbons by Carbon Nano-materials

KUN YANG[1,2], LIZHONG ZHU[2] and BAOSHAN XING[1,*]

[1]Department of Plant, Soil and Insect Sciences, University of Massachusetts, Amherst, Massachusetts 01003, USA
[2]Department of Environmental Science, Zhejiang University, Hangzhou, Zhejiang 310028, China
*Corresponding author phone: (413) 545-5212; fax: (413)545-3958; e-mail: bx@pssci.umass.edu.

Number of pages: 8

Number of figures: 6

Number of tables: 1

Figure S1 shows typical TEM images of fullerene and carbon nanotube aggregates.

Figure S2 shows solubility normalized adsorption isotherms of pyrene, phenanthrene and naphthalene.

Figure S3 shows the fits of Freundlich (FM), Langmuir (LM), Brunauer-Emmett-Teller (BET), Dual-mode (DMM), and Dual-Langmuir (DLM) models to the adsorption data of naphthalene, phenanthrene and pyrene on MWCNT15, while Figure S4 shows that of phenanthrene on fullerene, SWCNT and MWCNTs. Significant deviation of model fitting from the experimental data was observed for LM at high concentrations and for BET, DMM and DLM at relatively low concentrations. For FM, the goodness of fit varied with both the tested chemicals and carbon nano-sorbents. Good fits of FM were obtained for naphthalene on MWCNT15 and phenanthrene by SWCNT and fullerene, but not for others.

Figures S5 and S6 show empirical relationships between phenanthrene adsorption parameters of PMM and carbon nanotube properties. These relationships would be useful for estimating the parameters of PMM from carbon nano-material surface area, micropore volume and $R_{meso/micro}$.

Table SI lists the model fitting results of pyrene, phenantherene and naphthalene isotherms by nonlinear models, i.e., Freundlich (FM), Langmuir (LM), Brunauer-Emmett-Teller (BET), Dual-mode (DMM), Dual-Langmuir (DLM) and Polanyi-Manes (PMM) models.

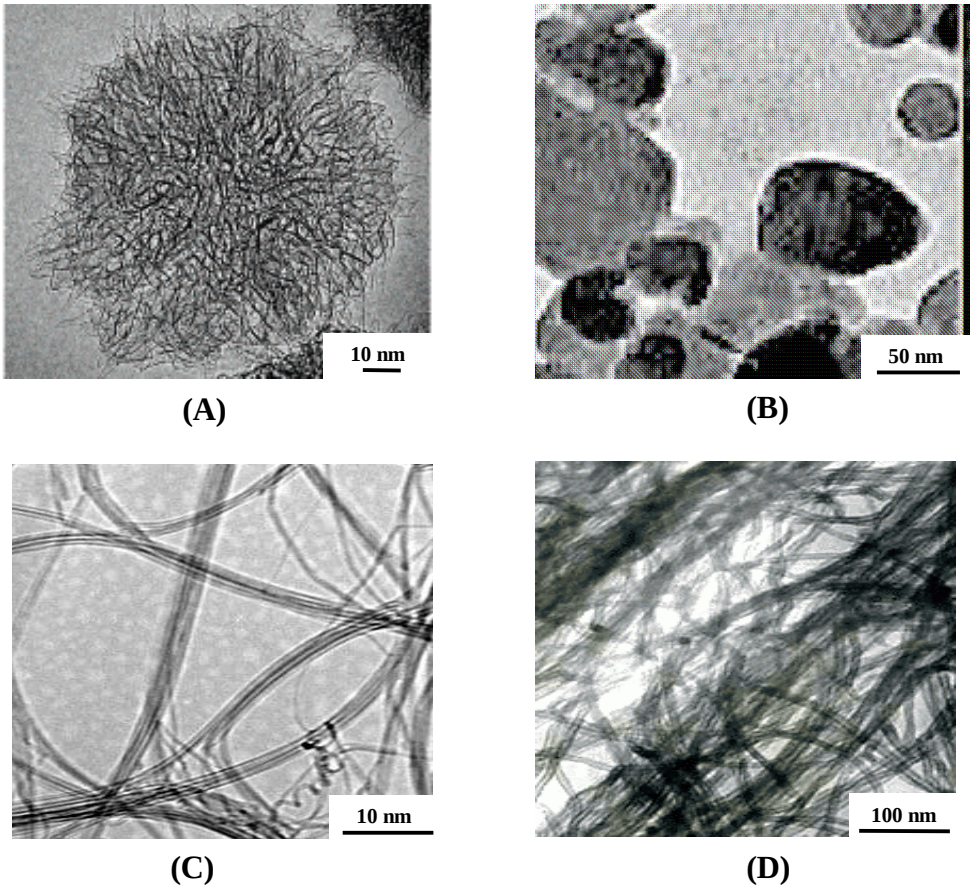

Figure S1, Typical TEM images of fullerene and carbon nanotube aggregates: (A) SWCNT aggregates from Yudasaka et al. (2005); (B) fullerene aggregates from Fortner et al. (2005); (C) part of SWCNT aggregate in this study and (D) part of MWCNT15 aggregate in this study.

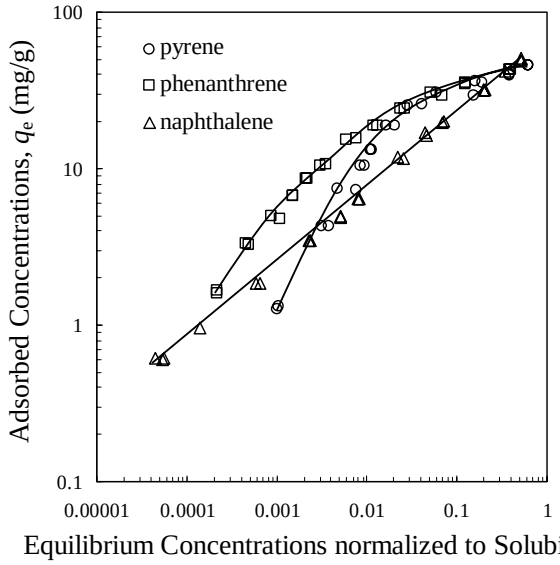

Figure S2, Solubility normalized adsorption isotherms of pyrene, phenanthrene and naphthalene by MWCNT 15

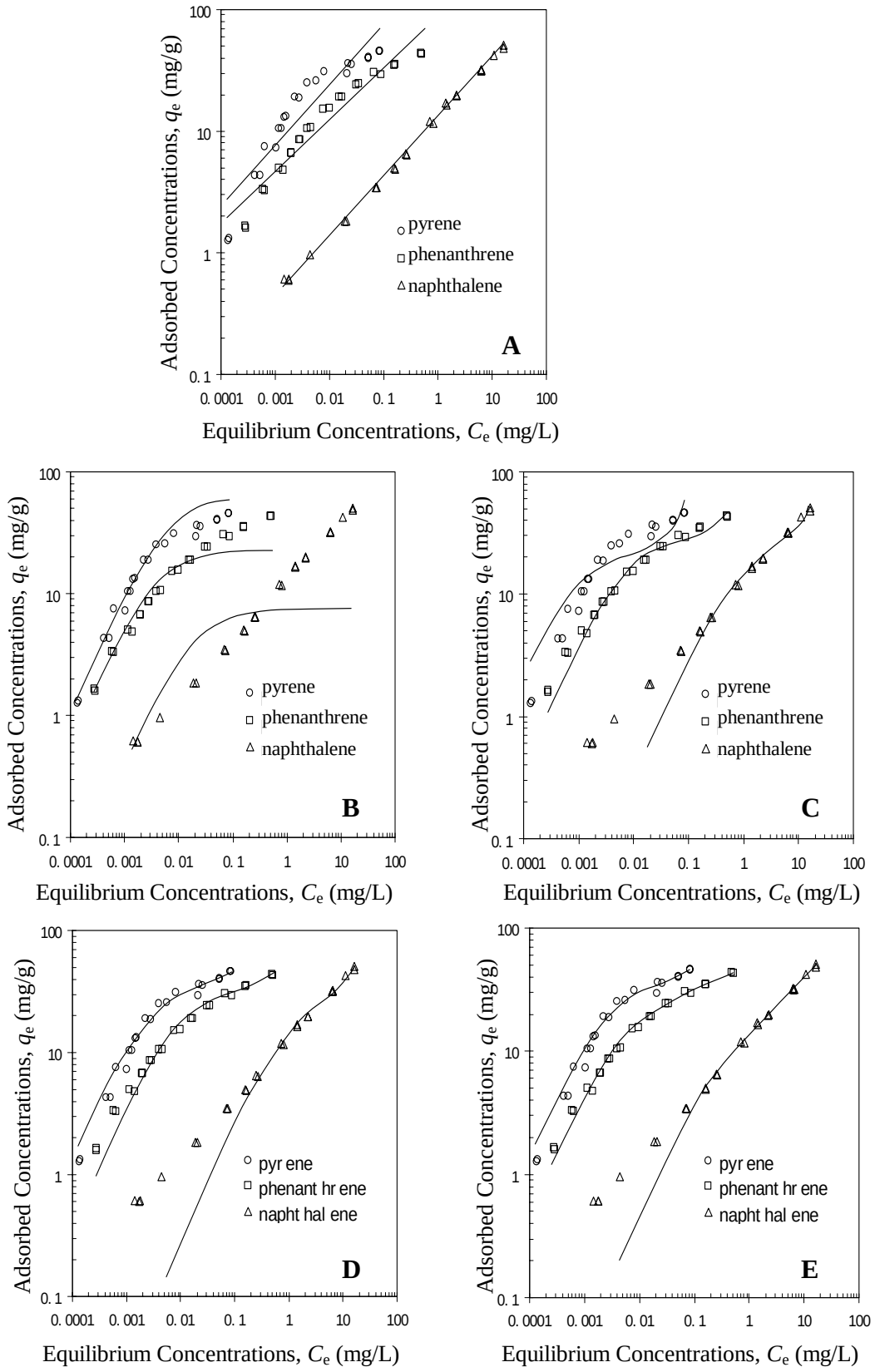

Figure S3, Model fits to adsorption data of pyrene, phenanthrene and naphthalene by MWCNT15. (A) Freundlich model (FM); (B) Langmuir model (LM); (C) Brunauer-Emmett-Teller model (BET); (D) Dual-mode model (DMM); and (E) Dual-Langmuir model (DLM).

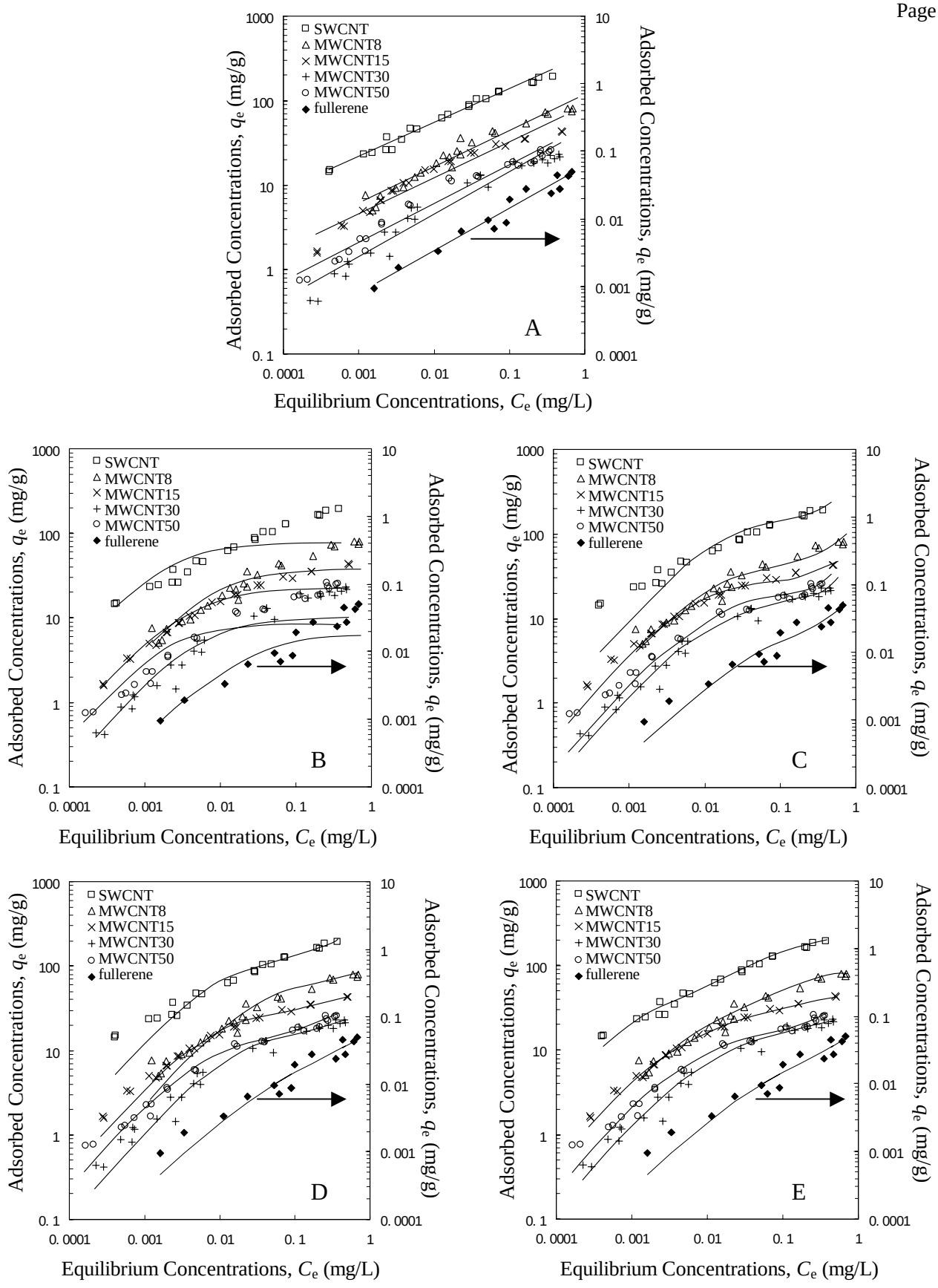

Figure S4, Model fits to adsorption data of phenanthrene by six carbon nano-materials. (A) Freundlich model (FM); (B) Langmuir model (LM); (C) Brunauer-Emmett-Teller model (BET); (D) Dual-mode model (DMM); and (E) Dual-Langmuir model (DLM). Right Y-axis is for fullerene and left Y-axis is for other sorbents.

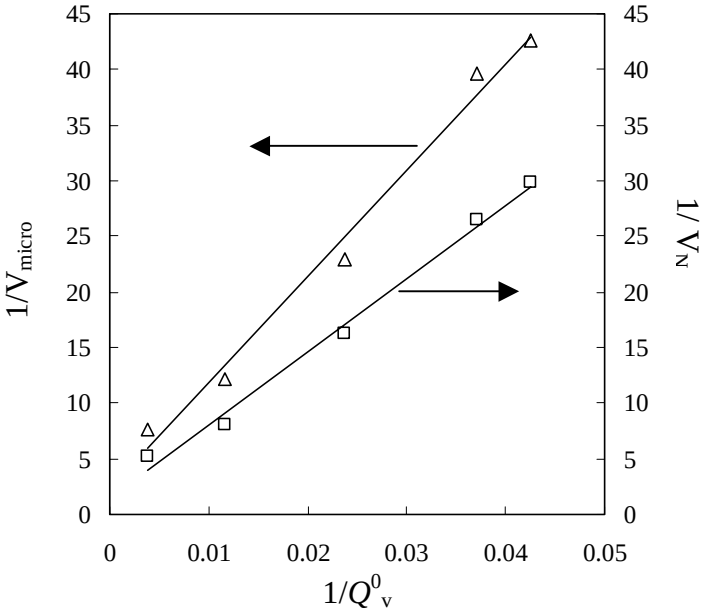

Figure S5. Plot of $1/V_{micro}$ or $1/V_N$ against $1/Q^0_V$. V_N is the mono-layer adsorption volume capacity of N_2; Q^0_v is the adsorbed volume capacity of phenanthrene estimated by PMM and V_{micro} is the micropore volume.

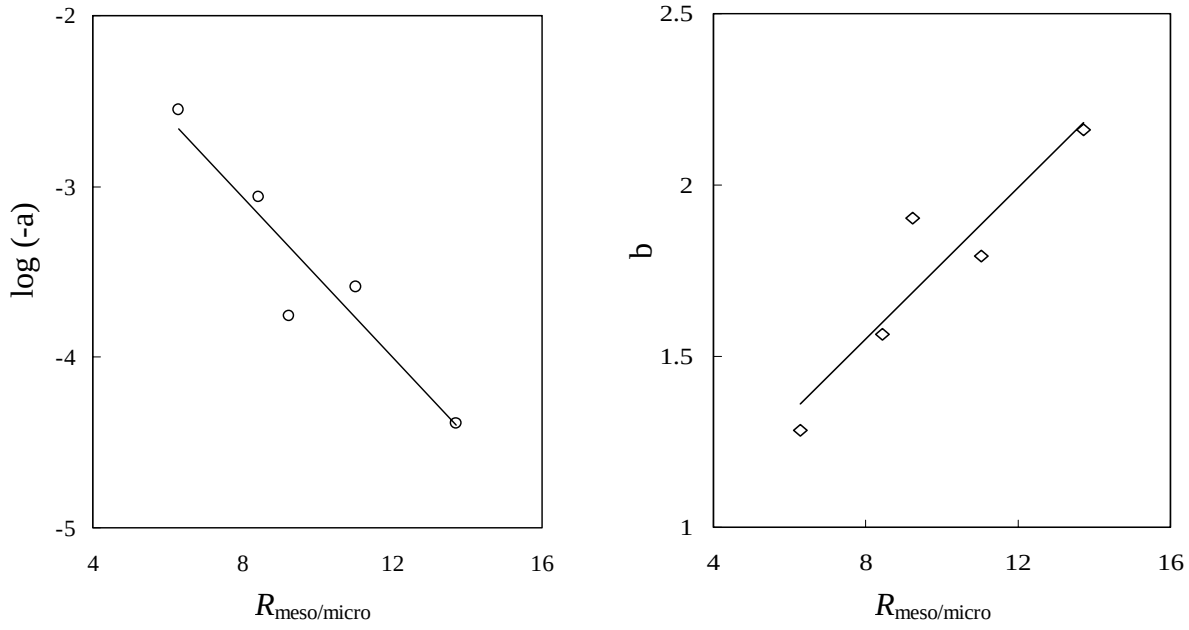

Figure S6. Plot of log(-a) or b vs. the ratios of mesopore to micropore volume ($R_{meso/micro} = V_{meso} / V_{micro}$) for carbon nanotubes.

Table SI. Results of Model Fits to Adsorption Isotherms of Pyrene, Phenanthrene and Naphthalene on Carbon Nanomaterials [a]

Freundlich Model (FM)

Carbons	compound	$\log K_f$	1/n	MWSE[b]	r^2	N[c]
Fullerene	phenanthrene	-1.24e+0±5.16e-2[d]	6.23e-1±3.74e-2	0.0737	0.959	14
SWCNT	phenanthrene	2.52e+0±2.30e-2	3.94e-1±1.10e-2	0.0116	0.985	22
MWCNT8	phenanthrene	2.07e+0±3.83e-2	4.30e-1±2.07e-2	0.0419	0.951	24
MWCNT15	naphthalene	1.11e+0±5.38e-3	4.85e-1±3.91e-3	0.00311	0.999	24
	phenanthrene	1.94e+0±5.44e-2	4.26e-1±2.39e-2	0.0864	0.936	24
	pyrene	2.37e+0±1.13e-1	4.98e-1±4.38e-2	0.228	0.866	22
MWCNT30	phenanthrene	1.68e+0±3.85e-2	4.56e-1±1.75e-2	0.0489	0.966	26
MWCNT50	phenanthrene	1.64e+0±4.87e-2	5.00e-1±2.28e-2	0.102	0.949	28

Langmuir Model (LM)

Carbons	compound	$1/Q^0$	K_d/Q^0	MWSE	r^2	N
Fullerene	phenanthrene	1.61e+0±6.80e-2	5.69e+1±1.27e+1	0.233	0.979	14
SWCNT	phenanthrene	2.50e-5±2.41e-6	1.33e-2±1.90e-3	0.166	0.843	22
MWCNT8	phenanthrene	2.14e-4±1.83e-5	2.68e-2±5.21e-3	0.109	0.862	24
MWCNT15	naphthalene	2.53e-3±1.49e-4	1.37e-1±3.31e-2	0.422	0.929	24
	phenanthrene	1.64e-4±3.76e-6	4.46e-2±4.39e-3	0.0550	0.989	24
	pyrene	1.03e-4±1.61e-6	1.58e-2±3.77e-3	0.0692	0.995	22
MWCNT30	phenanthrene	2.46e-4±1.61e-5	1.20e-1±2.65e-2	0.234	0.907	26
MWCNT50	phenanthrene	5.64e-4±2.44e-5	1.03e-1±3.04e-2	0.181	0.954	28

Brunauer-Emmett-Teller Model (BET)

Carbons	compound	Q^0	B	MWSE	r^2	N
Fullerene	phenanthrene	2.48e-2±2.06e-3	1.57e+1±7.14e+0	0.135	0.902	14
SWCNT	phenanthrene	1.43e+2±4.13e+0	8.73e+1±1.12e+1	0.103	0.974	22
MWCNT8	phenanthrene	4.30e+1±1.84e+0	1.02e+2±2.39e+1	0.0436	0.922	24
MWCNT15	naphthalene	2.62e+1±5.52e-1	3.74e+1±4.59e+0	0.210	0.988	24
	phenanthrene	2.85e+1±5.69e-1	1.88e+2±1.80e+1	0.0214	0.984	24
	pyrene	2.16e+1±1.33e+0	1.51e+2±6.43e+1	0.264	0.822	22
MWCNT30	phenanthrene	1.83e+1±4.18e-1	1.13e+2±1.70e+1	0.0621	0.978	26
MWCNT50	phenanthrene	1.55e+1±3.74e-1	1.02e+2±1.68e+1	0.0576	0.973	28

Dual-Mode Model (DMM)

Carbons	compound	K_P	Q^0	K_d	MWSE	r^2	N
Fullerene	phenanthrene	4.47e-2± 2.65e-2	1.82e-2± 2.00e-2	7.38e-2±1.44e-1	0.146	0.899	14
SWCNT	phenanthrene	2.54e+2± 3.12e+1	1.13e+2±7.57e+0	8.64e-3±1.63e-3	0.0676	0.982	22
MWCNT8	phenanthrene	2.84e+1± 9.44e+0	6.31e+1±5.68e+0	2.94e-2±5.36e-3	0.0705	0.978	24
MWCNT15	naphthalene	1.78e+0±1.06e-1	2.24e+1±1.49e+0	7.69e-1±1.24e-1	0.218	0.996	24
	phenanthrene	2.73e+1±2.61e+0	3.05e+1±8.92e-1	8.31e-3±6.95e-4	0.0334	0.993	24
	pyrene	1.22e+2± 3.09e+1	3.59e+1±2.02e+0	2.61e-3± 3.44e-4	0.0415	0.985	22
MWCNT30	phenanthrene	3.36e+1±3.73e+0	1.41e+1±9.52e-1	6.40e-3±1.33e-3	0.0311	0.985	26
MWCNT50	phenanthrene	1.33e+1±3.68e+0	1.68e+1±1.39e+0	1.60e-2±3.61e-3	0.0641	0.979	28

Dual-Langmuir Model (DLM)

Carbons	compound	Q_1^0	K_{d1}	Q_2^0	K_{d2}	MWSE	r^2	N
Fullerene	phenanthrene	1.82e-2±4.20e-2	7.38e-2±2.34e-1	7.54e+4±2.50e+11	1.69e+6±5.61e+12	0.161	0.899	14
SWCNT	phenanthrene	4.04e+1±7.86e+0	1.24e-3±6.12e-4	1.82e+2±6.95e+0	8.05e-2±1.50e-2	0.0180	0.993	22
MWCNT8	phenanthrene	1.97e+1±9.16e+0	5.37e-3±4.15e-3	6.97e+1±6.81e+0	1.22e-1±5.10e-2	0.0270	0.984	24
MWCNT15	naphthalene	1.28e+1±1.48e+0	2.98e-1±6.77e-2	8.22e+1±7.90e+0	1.98e+1±4.26e+0	0.178	0.998	24
	phenanthrene	2.21e+1±1.60e+0	4.88e-3±6.06e-4	2.84e+1±1.39e+0	1.68e-1±3.98e-2	0.0123	0.997	24
	pyrene	3.59e+1±2.15e+0	2.61e-3±3.55e-4	8.99e+7±1.91e+14	7.35e+5±1.56e+12	0.0438	0.985	22
MWCNT30	phenanthrene	1.41e+1±9.79e-1	6.40e-3±1.37e-3	2.88e+9±5.00e+15	8.58e+7±1.49e+14	0.0325	0.985	26
MWCNT50	phenanthrene	1.05e+1±5.46e+0	8.52e-3±5.56e-3	1.52e+1±3.48e+0	1.46e-1±1.53e-1	0.0579	0.980	28

Polanyi-Manes Model (PMM)

Carbons	compound	$\log Q^0$	a	b	MWSE	r^2	N
Fullerene	phenanthrene	-1.17e+0±1.52e-1	-1.82e-2±1.85e-2	1.00e+0±2.11e-1	0.0797	0.959	14
SWCNT	phenanthrene	2.42e+0±4.93e-2	-2.78e-3±1.60e-3	1.28e+0±1.15e-1	0.00941	0.989	22
MWCNT8	phenanthrene	1.94e+0±4.10e-2	-8.64e-4±6.05e-4	1.56e+0±1.49e-1	0.0230	0.974	24
MWCNT15	naphthalene	1.87e+0±2.30e-2	-1.31e-2±1.82e-3	9.68e-1±2.51e-2	0.00298	0.999	24
	phenanthrene	1.62e+0±1.39e-2	-4.11e-5±1.30e-5	2.16e+0±6.50e-2	0.00330	0.997	24
	pyrene	1.63e+0±2.26e-2	-1.35e-5±8.01e-6	2.49e+0±1.28e-1	0.0170	0.988	22
MWCNT30	phenanthrene	1.43e+0±3.18e-2	-2.58e-4±1.57e-4	1.79e+0±1.25e-1	0.0203	0.989	26
MWCNT50	phenanthrene	1.37e+0±3.60e-2	-1.74e-4±1.21e-4	1.90e+0±1.44e-1	0.0458	0.983	28

[a] Linear regression was employed for Freundlich and Langmuir models; Nonlinear regression was employed for BET, DMM, DLM and PMM models; All estimated parameter values and their standard errors were determined by commercial software program (SPSS10.0 or sigmaplot). [b] MWSE is mean weighted square error, equal to $1/v[(q_{measured} - q_{model})^2/q^2_{measured}]$, where v is the amount of freedom; v=N-2 for Freundlich, Langmuir and BET models, v=N-3 for DMM and PMM models, v=N-4 for DLM model. [c] N=number of observations. [d] Mean±standard deviation.

Literature cited:

Fortner, J.D., Lyon, D.Y., Sayes, C.M., Boyd, A.M., Falkner, J.C., Hotze, E.M., Alemany, L.B., Tao, Y.J., Guo, W., Ausman, K.D., Colvin, V.L., Hughes, J.B., 2005. C_{60} in Water: Nanocrystal formation and microbial response. Environ. Sci. Technol. 39, 4307-4316.

Yudasaka, M., Fan, J., Miyawaki, J., Iijima, S., 2005. Studies on the adsorption of organic materials inside thick carbon nanotubes. J. Phys. Chem. B 109, 8909-8913.